Diagnosis of Physical Conditions in Herbig-Haro Objects

Author: Astrid Algarra Santos.
Advisor: Maria Rosario López Hermoso
Facultat de Física, Universitat de Barcelona, Martí i Franquès 1, 08028 Barcelona, Spain.*

Abstract: Herbig-Haro object spectrophotometry allows us to determine some of their physical conditions (degree of excitation and tracers of electron density, electron temperature and degree of ionization) through the calculation of line ratios for some of the forbidden lines in the optical spectrum. The aim of this work is to search for optical spectra of HHs of the Orion star-forming region and use them to perform diagnosis on these properties.

I. INTRODUCTION

Mass ejection at high speeds (of the order of hundreds of km s^{-1}) is a phenomenon associated with the star formation process, which is observed in the optical and infrared spectrum via stellar jets. The protostars are formed within molecular clouds as the result of the gravitational collapse of dense cores. First, matter accumulates on the accretion disc and, due to viscosity, it loses energy and falls onto the protostar. The protostar can't absorb all the matter that falls onto it from the accretion disc and ejects a fraction of it. The ejected material is collimated by the disc via mechanisms outside the scope of this work. This produces, on the one hand, low-collimated molecular outflows, traveling at speeds of the order of tens of km s^{-1}, observed in the emission lines of the CO molecule and, on the other, the high-collimated stellar jets, traveling at speeds of the order of hundreds of km s^{-1}, observed in the optical and infrared spectrum.

In the fifties, George Herbig and Guillermo Haro discovered a series of nebular emissions in the star-forming region of Orion that were not associated with any star. These were named Herbig-Haro objects or HH. It was later observed that these objects were aligned in strings of knots forming what is called a stellar jet, characterized by its highly collimated morphology. The knots are formed due to the interaction of high speed material with the previously ejected material producing shocks in the collision zone. The gas heated in the collisions is cooled via radiation, emitting lines which can be permitted or forbidden depending on whether or not they follow the electrical dipole selection rules. The forbidden lines are characteristic of low density media (10^4 - 10^5 cm^{-3}), typical of the jets.

The goal of this work is to use different line ratios, characteristic of these jets, to determine physical conditions of the HH objects. We'll use the most characteristic lines on the optical spectrum of Herbig-Haro objects (Hβ, [O III] λ 5007 Å, [O I] λ 6300, 6364 Å, [N II] λ 6548, 6583 Å, Hα and [S II] λ 6716, 6731 Å) to diagnose their physical conditions.

II. DATA COLLECTION

The data presented in this work belong to HH objects located in the Orion nebula, a low and high mass star formation region. These data include fluxes from the different lines in which we are interested and were collected from various sources. This work is composed of two main parts: the identification of HH objects in the nebula and, for each of those, the search and homogenization of their line fluxes.

In order to identify the objects we used the Reipurth catalogue, obtained with the VIZIER database, accessed via the CDS website [1], which is a compilation of every known HH jet. We selected those belonging to Orion based on their coordinates, identifying a total of 142 jets. We then selected a sample of 30 objects including only those who had published accessible spectra.

We then proceeded the search for fluxes for these objects. The paper "A Compilation of Optical Spectrophotometry of HH Objects and its Tentative Interpretation" [2] contains a database of line fluxes collected up to 1996, which acted as our starting point. Next, we searched papers containing relevant spectral data of the objects in our sample using the SIMBAD database [1], limiting our search to those published between 1997 and 2018. Because line fluxes are collected from different sources, the data are heterogeneous (e.g. extinction corrected or not, flux calibrated or not, flux normalized to Hα or Hβ). During the process, we have chosen to favor the more recent data. In those cases in which data from the same epoch were available, we favored those which were extinction corrected. We then normalized the data to Hβ = 100. The resulting database is shown in Table I.

III. RESULTS

Using the fluxes collected in Table I we performed a diagnosis of physical conditions in the objects. The line ratios used are: [S II] 6716/6731 to obtain the tracer of electron density (n_e), [N II]/[O I] 6584/6300 to obtain the tracer of degree of ionization (χ_e), [O I]/[S II] (6300+6364)/(6716+6731) to obtain the tracer of electron temperature (T_e), [O III] 5007/Hβ and [S II] (6716+6731)/Hα to obtain the degree of excitation, which is a tracer of the strength of the shock.

We have classified the objects according to the excitation degree of their spectrum (high, intermediate or low), using the criteria given in [2]:

i) “high excitation spectra”, with [O III] 5007/Hβ > 0.1 and [S II] (6716+6731)/Hα ≤ 1.5,

ii) “intermediate excitation spectra”, with [O III] 5007/Hβ ≤ 0.1 and [S II] (6716+6731)/Hα ≤ 1.5,

iii) “low excitation spectra”, with [O III] 5007/Hβ ≤ 0.1 and [S II] (6716+6731)/Hα > 1.5.

Results are shown in a bidimensional histogram Fig.(1) for both ratios ([O III] 5007/Hβ and [S II] (6716+6731)/Hα) representing the amount of objects found for each combination of values. The histogram can be divided into four regions: one for each rate of excitation and a forbidden zone, in which no objects should be found.

We have used the diagnostic diagrams given in [2] and [3] to represent the line ratios obtained for the objects of our sample (Fig.(2) and Fig.(3)).

* Electronic address: aalgarsa8@alumnes.ub.edu

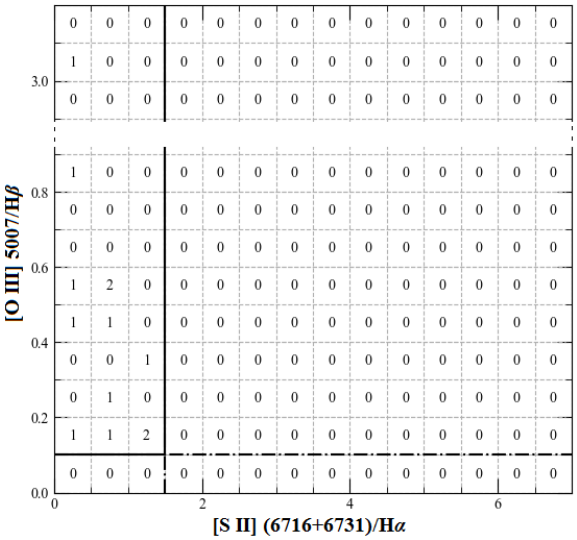

FIG. 1: Graph showing the [O III] 5007/Hβ vs. [S II] (6716+6731)/Hα. Low excitation objects are found below [O III] 5007/Hβ = 0.1, high excitation ones are found to the left of [S II] (6716+6731)/Hα = 1.5 and intermediate excitation ones are found in the intersection of both (following the structure presented in [2]).

In Fig.(2) we represent Hα/[S II] (6716+6731) vs. Hα/[N II] (6548+6583), which are tracers of excitation.

In Fig.(3) we represent the tracers of electron density vs. excitation. From this diagram, the degree of excitation can be obtained, just as with the bidimensional histogram (Fig.(1)). This allows us to classify those objects for which the flux for the [O III] λ 5007 Å line was not available.

In Fig.(4) we show a couple of histograms: one for the decimal logarithm of the tracer of electron temperature ([O I]/[S II] (6300+6364/6716+6731)) and another for the decimal logarithm of the tracer of degree of ionization ([N II]/[O I] (6584/6300)).

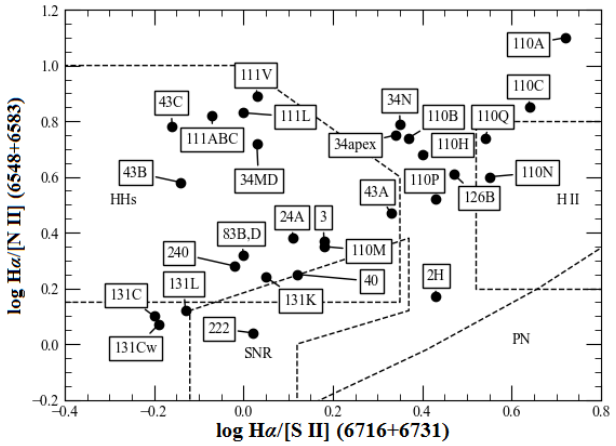

FIG. 2: Position of the objects in a diagnostic diagram of log (Hα/[N II] (6548+6583)) vs. log (Hα/[S II] (6716+6731)). The regions of the Planetary Nebulae (PN), Supernova Remnants (SNR), H II regions (H II) and Herbig-Haro objects (HHs) are outlined using figures of [3].

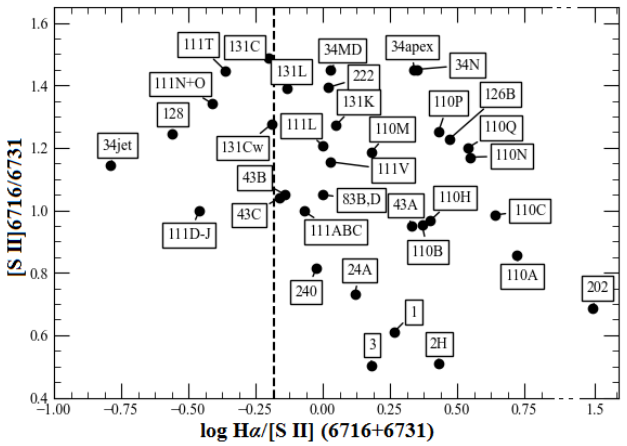

FIG. 3: Position of the objects in the tracer of electron density vs. excitation diagnostic diagram. The long-dashed line gives the separation between high/intermediate (right) and low (left) excitation HH spectra (as proposed in [2]).

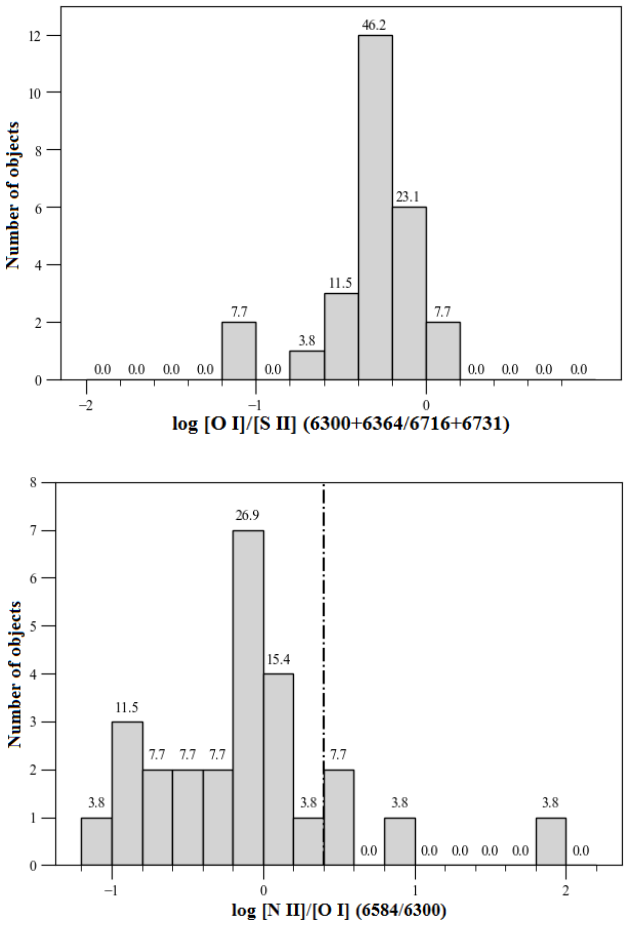

FIG. 4: Histograms showing the distribution for the logarithm of the tracer of electron temperature [O I]/[S II] (top) and for the logarithm of the tracer of degree of ionization [N II]/[O I] (bottom). The percentage of objects in each bin is shown above the corresponding bar. The values on the right side of the vertical line in bottom one correspond to the objects with a very high degree of ionization (> 60%).

IV. DISCUSSION

As we have seen in Fig.(1) and Fig.(3), high excitation objects are prevalent in our sample. In Fig.(1) all the represented objects (13) are found inside the high excitation region, because none of the ones which would fall in the low or intermediate excitation areas had available data for the [O III] λ 5007 Å line. However, based on the Hα/[S II] (6716+6731) ratio we can assume that 4 of those would fall on the low excitation region. In the case of Fig.(3), we found that the distribution was: 14% low excitation, 14% intermediate excitation and 71% high excitation spectra. This prevalence is due to the selected region's properties; it would be interesting to compare these percentages to those of a region with different properties, e.g. the Taurus nebula, a low mass star formation region.

In Fig.(2) we see that most of the plotted objects fall within the expected region (14) or close to its borders (11). However, we count four objects located far from this area of the graph; these are all knots belonging to HH 110, which stray progressively toward the right side. This behavior could be related to the effects of the interaction with its neighbor, HH 270, which appears to be moving toward HH 110 producing deflection in the latter [4]. There is also a special case, HH 202, which isn't shown in the graph because of its peculiarly high excitation. We found that this object's tracer of degree of is also particularly greater than expected. In this case, photoionization effects should be an important contributor and the tracer we use is not fully appropriate

We now presents a tables with some statistic results extracted from the data with which we composed the histograms in Fig.(4). We have discarded the values for objects which showed a very high degree of ionization (HH 126B, HH 131Cw, HH 202, HH 222) because, in these objects, collision is not the predominant mechanism in determining line fluxes (the resulting emission is affected by radiation of neighboring stars) and the model [5] used to calculate the actual values from their tracers wouldn't work in these conditions.

The estimated values for T_e and χ_e, according to the models [5], and for n_e, calculated using the IRAF [6][1] are given in Table III.

	[O I]/[S II] (T_e)	[N II]/[O I] (χ_e)	[S II] 6716/6731 (n_e)
Average	0.66	0.69	1.08
Standard deviation	0.28	0.50	0.30
Minimum	0.28	0.04	0.50
Maximum	1.46	1.97	1.49

TABLE II: Statistical values obtained for the tracers of electron temperature, degree of ionization and electron density.

	T_e (10^4 K)	χ_e (%)	n_e (cm^{-3})
Average	1.2	35	400
Minimum	0.3	5	< 10
Maximum	> 1.5	> 60	13,200

TABLE III: Average values and ranges obtained for each magnitude.

V. CONCLUSIONS

- We found that in the Orion region high excitation HH objects are prevalent, representing over 70% of the HH population. We also corroborated the effects of irradiation in several on these objects' emission spectra.
- Regarding the collection of data, about 500 papers were consulted. This shows the difficulty of performing a statistical study of the physical conditions of these objects due to the lack spectroscopic observations database.

VI. APPENDIX

We now present the table with the collected data for the line fluxes of the different objects, in order of right ascension. Due to its large size, it is presented in its own page.

[1] "IRAF is distributed by the National Optical Astronomy Observatories, which are operated by the Association of Universities for Research in Astronomy, Inc., under cooperative agreement with the National Science Foundation"

TABLE I

FLUXES OF HH OBJECTS RELATIVE TO Hβ = 100

HH	R.A.(J2000) ($^h\,^m\,^s$)	Decl.(J2000) (° ′ ″)	[O III] λ 5007 Å	[O I] λ 6300 Å	[O I] λ 6364 Å	[N II] λ 6548 Å	Hα λ 6563 Å	[N II] λ 6583 Å	[S II] λ 6716 Å	[S II] λ 6731 Å
240	05 19 40.8	-05 51 44	33	374	…	…	578	230	274	336
83B,D	05 33 31.7	-06 29 38	11	119	…	…	288	103	148	141
131Cw	05 33 49.0	+08 42 46	…	22	20	26	122	77	106	83
131C	05 33 51.4	+08 42 38	…	…	…	44	256	159	244	164
131K	05 34 19.3	+08 32 01	…	…	…	23	141	59	70	55
131L	05 34 27.1	+08 34 24	…	74	…	49	256	146	203	146
202	05 35 11.5	-05 22 46	304	0.5	0.2	16	279	47	4	5
126B	05 35 26.8	-06 22 46	16	21	…	…	290	54	54	44
34jet	05 35 31.3	-06 28 43	…	1235	…	…	409	48	1335	1165
34MD	05 35 31.3	-06 28 43	14	119	40	…	389	55	216	149
34apex	05 35 31.3	-06 28 43	52	53	18	…	354	47	96	67
40	05 35 31.6	-06 28 36	60	76	…	…	214	91	…	…
34N	05 35 31.7	-06 24 26	…	83	28	…	453	55	119	82
222	05 35 41.0	-06 23 00	…	23	8	68	354	217	195	140
128	05 36 08.5	-05 04 38	…	306	…	…	275	32	552	444
3	05 36 11.7	-06 43 04	44	67	…	…	285	92	63	125
1	05 36 20.8	-06 45 13	57	159	…	…	311	151	64	105
2A	05 36 25.3	-06 47 10	109	110	…	…	335	115	64	…
2H	05 36 25.5	-06 47 15	81	138	50	47	343	182	43	85
2G	05 36 25.9	-06 47 09	35	149	…	…	278	116	83	…
43A	05 38 10.8	-07 09 23	48	97	…	…	341	86	77	81
43B	05 38 10.8	-07 09 23	…	287	…	…	480	95	336	320
43C	05 38 10.8	-07 09 23	…	476	…	…	526	66	391	376
24A	05 46 09.2	-00 10 26	22	103	…	…	228	72	74	101
111V	05 51 36.5	+02 48 48	…	99	…	…	298	29	149	129
111L	05 51 36.5	+02 48 48	10	136	…	…	298	33	163	135
111D-J	05 51 36.5	+02 48 48	…	540	…	…	407	84	580	582
111N+O	05 51 36.5	+02 48 48	…	354	118	…	408	34	598	446
111ABC	05 51 36.5	+02 48 48	…	284	95	…	500	57	293	294
111T[a]	05 51 36.5	+02 48 48	…	63	21	…	100	…	136	94

[a]Normalized to Hα = 100 because the flux of Hβ was not available.

240, 83, 40, 126B, 34jet, 128, 3, 1, 2A, 2G, 43A, 43B, 43C, 24A, 111V, 111L, 111D-J : [2]
131C, 131L, 131K, 131Cw : [7]
202: [8]
34MD, 34apex: [9]
34N, 111N+O, 111ABC, 111T: [10]
222: [11]
2H: [12]
110A, 110B, 110C, 110H, 110M, 110N, 110P, 110Q: [13], do not show up in the table due to lack of line fluxes but their ratios were used.

Acknowledgments

I'd like to thank God for the people He sent me to stand by me and help me during the realization of this work: my advisor, Rosario López, for her patience and commitment, to Sebastián Hernández, who was there for me for the last three years, and my family.

---

[1] "Strasbourg Astronomical Data Center," [Online]. Available: http://vizier.u-strasbg.fr. [Accessed 2018].

[2] A. C. Raga, K.-H, Bohm and J. Cantó, "A Compilation of Optical Spectrophotometry of HH Objects and Its Tentative Interpretation," *Rev. Mex. Astron. Astrofis.*, no. 32, pp. 161-174, 1996.

[3] J. Cantó, in *Investigating the Universe*, Dodrecht:Reidel, F. Khan, 1981, p. 95.

[4] B. Reipurth and J. Bally, "Herbig-Haro Flows: Probes of Early Stellar Evolution," *Annu. Rev. Astron. Astrophys.*, no. 39, pp. 403-455, 2001.

[5] L. Podio, S. Medves, F. Bacciotti, J. Eislöffel and T. Ray, "Physical Structure and Dust Reprocessing in a Sample of HH Jets," *Astronomy & Astrophysics*, no. 506, pp. 779-788, 2009.

[6] "the Image Reduction and Analysis Facility," [Online]. Available: http://iraf.noao.edu/. [Accessed 2018].

[7] M. Wang, J. Noumaru, H. Wang, J. Yang and J. Chen, "The Intriguing Giant Bow Shocks Near HH 131," *The Astronomical Journal*, no. 130, p. 2745–2756, 2005.

[8] A. Mesa-Delgado, C. Esteban, J. García-Rojas, V. Luridiana, M. Bautista, M. Rodríguez, L. López-Martín and M. Peimbert, "Properties of the Ionized Gas in HH 202 – II. Results from Echelle Spectrophotometry with Ultraviolet Visual Echelle Spectrograph," *Mon. Not. R. Astron. Soc.*, no. 395, p. 855–876, 2009.

[9] M. A. Dopita and R. S. Sutherland, "Effects of Pre-Ionisation in Radiative Shocks II: Application to the Herbig-Haro Objects," *Draft version*, 2017.

[10] J. A. Morse, S. Heathcote, P. Hartigan and G. Cecil, "Spectrophotometric Evidence for Velocity Variability in the HH 34 and HH 111 Stellar Jets," *The Astronomical Journal*, vol. 106, no. 3, pp. 1139-1155, 1993.

[11] B. Reipurth, J. Bally, C. Aspin, M. S. Connelley, T. R. Geballe, S. Kraus, I. Appenzelle and A. Burgasser, "HH 222: a Giant Herbig–Haro Flow from the Quadruple System V380 Ori," *The Astronomical Journal*, no. 11pp, pp. 146-118, 2013.

[12] R. D. Schwartz, "Herbig-Haro Objects," *Ann. Rev. Astron. Astrophys.*, no. 21, pp. 209-237, 1983.

[13] B. Reipurth, A. Raga and S. Heathcote, "HH 110: the Grazing Collision of a Herbig-Haro Flow with a Molecular Cloud Core," *Astron. Astrophys.*, no. 311, pp. 989-996, 1996.